International Journal of Thermal Sciences 48 (2009) 1405–1415

Contents lists available at ScienceDirect

International Journal of Thermal Sciences

www.elsevier.com/locate/ijts

Natural convection in a diagonally divided square cavity filled with a porous medium

Yasin Varol [a], Hakan F. Oztop [a], Ioan Pop [b,*]

[a] Department of Mechanical Education, Firat University, TR-23119, Elazig, Turkey
[b] Faculty of Mathematics, University of Cluj, R-3400 Cluj, CP 253, Romania

ARTICLE INFO

Article history:
Received 3 September 2008
Received in revised form 18 December 2008
Accepted 19 December 2008
Available online 17 January 2009

Keywords:
Divided cavity
Natural convection
Porous medium
Numerical results

ABSTRACT

The flow and heat transfer in a diagonally divided square cavity by an inclined plate and filled with a porous medium were numerically analyzed in this paper. Vertical walls are kept at isothermal conditions, while horizontal walls are insulated. A finite difference scheme was used to solve the dimensionless governing partial differential equations along with the corresponding boundary conditions. Computations were carried out to examine the effects of Rayleigh number ($100 \leqslant Ra \leqslant 1000$), thermal conductivity ratio between plate and fluid ($0.1 \leqslant k \leqslant 10$) and the position of the partition (45°, Case I and 135°, Case II). It was found that heat transfer is attenuated when the plate is positioned at 45°, the heat transfer is less than when it is at 135°.

1. Introduction

Natural convection heat transfer in a cavity filled with fluid saturated porous media can be seen in many applications of engineering. Some of these are solar power collectors, geothermal applications, nuclear reactors and so on. Detailed reviews of the subject of porous media can be found in the well documented books as Nield and Bejan [1], Ingham and Pop [2], Vafai [3], Pop and Ingham [4], Bejan et al. [5] and Vadasz [6].

Dividers are used to control the convective flows in cavities, which have many engineering applications. The heat transfer rate through the system with partitions decreases. The types of divided cavities with partitions can be classified in three groups: (a) fully divided horizontal or vertical cavities with partition/partitions [7–9], (b) divided cavities with partial partitions [10–13] and (c) divided cavities with inclined partitions [14–17]. But studies on control of natural convection heat transfer via partitions are very limited for cavities filled with porous media.

Tong and Gerner [7] made a numerical study on natural convection in partitioned square cavities with a vertical partition and filled with air and found that partitioning is an effective method of reducing heat transfer. Maximum reduction in heat transfer occurs when the partition is placed midway between the vertical walls. Ho and Yih [8] made an analysis of heat transfer for a vertically partitioned cavity filled with air. They showed that the heat transfer rate is considerably attenuated in a partitioned cavity in comparing with that for non-partitioned cavity. Nishimura et al. [9] performed a similar work for tall cavities. Turkoglu and Yucel [10] searched the effects of number of vertical partitions on natural convection inside cavities. Chen et al. [11] investigated the effects of the partitions in open cavities, while Bilgen [12] studied the laminar and turbulent convection in cavities with partial partitions. Bilgen [12] found that for a small aspect ratio the heat transfer is reduced when two partitions were used instead of one partition. Oztop and Dagtekin [13] modeled the electronical devices using two heated partitions at different dimensions. Nanstell and Greif [14,15] made experiments on a two-dimensional scale model having an aspect ratio of 0.5 and a partition hanging from the top wall. They observed that the flow was essentially laminar, turbulence on the vertical walls seemed to be suppressed by the partitions.

It seems that the first studies on natural convection in porous triangular cavities divided by solid fins or an embedded solid horizontal plate were made by Varol et al. [16,17]. They observed that the solid partitions affect the flow and temperature fields as well as the heat transfer. Then Saeid [18,19] solved the conjugate natural convection in thick walled cavities filled with fluid saturated porous media. He also found that heat transfer is a function of Rayleigh number, thickness of partition and thermal conductivity ratio between wall and fluid. The conjugate conduction-forced convection in a plane channel filled with a saturated porous medium is investigated analytically by Nield and Kuznetsov [20].

Ben-Nakhi and Chamkha [21] focused on the numerical study of steady, laminar, conjugate natural convection in a square enclo-

* Corresponding author. Tel.: +40 264 594315; fax: +40 264 591906.
E-mail address: pop.ioan@yahoo.co.uk (I. Pop).

1290-0729/$ – see front matter
doi:10.1016/j.ijthermalsci.2008.12.015

Nomenclature

g	gravitational acceleration	m/s^2
H	height of the cavity	m
K	permeability of the porous medium	m^2
L	length of the cavity	m
Nu_y	local Nusselt number	
Nu	mean Nusselt number	
n	normal coordinate	
Ra	Rayleigh number	
T_f	temperature of the fluid-saturated porous medium	K
T_s	temperature of the conductive solid inclined plate	K
u, v	dimensional velocities	m/s
U, V	dimensionless velocities	
x, y	dimensional coordinates	m
X, Y	dimensionless coordinates	

Greek letters

α_m	effective thermal diffusivity	m^2/s
β	thermal expansion coefficient	K^{-1}
θ	dimensionless temperature	
υ	kinematic viscosity	m^2/s
Ψ	dimensionless stream function	

Subscripts

C	cold
H	hot
f	fluid
s	solid

sure with an inclined thin fin of arbitrary length. In their study, the inclined fin is attached to the left thin vertical wall of the cavity, while the other three sides are considered to have finite and equal thicknesses of arbitrary thermal conductivities. It was found that the inclination of the thin fin and the thermal conductivity ratio of the solid-to-fluid have significant effects on the local and average Nusselt number. Then, similar problem was extended to solve the conjugate problem with inclined partition by same authors [22]. Mezrhab et al. [23] made a numerical work to analyze the effects of single and multiple partitions on heat transfer phenomena in an inclined square cavity using lattice-Boltzmann technique. They investigated the effects of inclination angles and gap width and observed that the mean Nusselt number decreases when the number of partitions attached to the cold wall of the enclosure increases. Jami et al. [24] studied numerically the laminar natural convection heat transfer in a differentially heated inclined cavity with partitions attached to its hot wall. They used the hybrid lattice-Boltzmann finite-difference method. It was shown that the heat transfer increases with increasing the length of the dimensionless partition. Recently, Sahin and Arici [25] analyzed the natural convection in fully divided cavities filled with clear fluids (non-porous media) by considering all possible locations including the orthogonal location.

The main objective of the present study is to illustrate the effects of diagonally inserted conductive thin plate on natural convection flow in a cavity filled with a porous medium. The searched literature showed that the model has not been tested in earlier studies. Thus, it is proposed to show that the buoyancy induced heat transfer and fluid flow can be controlled and that the obtained results can be used for engineers and thermal designers. Numerical results are obtained for an inclined partition in a two-dimensional square cavity filled with a porous medium as shown in Fig. 1(a) for a partition connecting the upper right corner with the lower left corner or when the conductive plate is inclined at 45° (Case I) and Fig. 1(b) for a partition connecting the upper left corner with the lower right corner or when the conductive plate is inclined at 135° (Case II), respectively. An acceptable formula can be $\phi = than^{-1}(CI)$, where $CI = 1$ and -1 for Cases I and II, respectively. The thickness of the inclined conductive plate is accepted as thin. The dimensions of height and length are equal as $H = L$. The vertical walls are isothermal but temperature of the left wall is higher than that of the right wall. The horizontal walls are adiabatic. Thermal conductivity ratio is defined as $k = k_f/k_s$ between fluid and inclined solid plate.

2. Mathematical model

In order to write the governing equations for the problem under consideration the following assumptions are made: the properties of the fluid and the porous medium are constant; the cavity walls are impermeable; the Boussinesq approximation and the Darcy law model are valid. With these assumptions, the dimensional governing equations as continuity, momentum, and energy can be written as follows

$$\frac{\partial u}{\partial x} + \frac{\partial v}{\partial y} = 0 \tag{1}$$

$$\frac{\partial u}{\partial y} - \frac{\partial v}{\partial x} = -\frac{g\beta K}{\upsilon}\frac{\partial T_f}{\partial x} \tag{2}$$

$$u\frac{\partial T_f}{\partial x} + v\frac{\partial T_f}{\partial y} = \alpha_m\left(\frac{\partial^2 T_f}{\partial x^2} + \frac{\partial^2 T_f}{\partial y^2}\right) \tag{3}$$

and the energy equation for the two-dimensional inclined plate is:

$$\frac{\partial^2 T_s}{\partial x^2} + \frac{\partial^2 T_s}{\partial y^2} = 0 \tag{4}$$

where u and v are the velocity components along x- and y-axes, T_f is the fluid temperature, g is the acceleration due to gravity, T_s is the temperature of the inclined solid plate, K is the permeability of the porous medium, α_m is the effective thermal diffusivity of the porous medium, β is the thermal expansion coefficient and υ is the kinematic viscosity. Introducing the stream function ψ defined as

$$u = \frac{\partial \psi}{\partial y}, \qquad v = -\frac{\partial \psi}{\partial x} \tag{5}$$

Eqs. (1)–(4) can be written in non-dimensional form as

$$\frac{\partial^2 \Psi}{\partial X^2} + \frac{\partial^2 \Psi}{\partial Y^2} = -Ra\frac{\partial \theta_f}{\partial X} \tag{6}$$

$$\frac{\partial \Psi}{\partial Y}\frac{\partial \theta_f}{\partial X} - \frac{\partial \Psi}{\partial X}\frac{\partial \theta_f}{\partial Y} = \frac{\partial^2 \theta_f}{\partial X^2} + \frac{\partial^2 \theta_f}{\partial Y^2} \tag{7}$$

for the fluid-saturated porous medium and

$$\frac{\partial^2 \theta_s}{\partial X^2} + \frac{\partial^2 \theta_s}{\partial Y^2} = 0 \tag{8}$$

for the inclined plate, respectively. Here $Ra = g\beta K(T_H - T_C)L/\alpha_m\upsilon$ is the Rayleigh number for the porous medium and the non-dimensional quantities are defined as

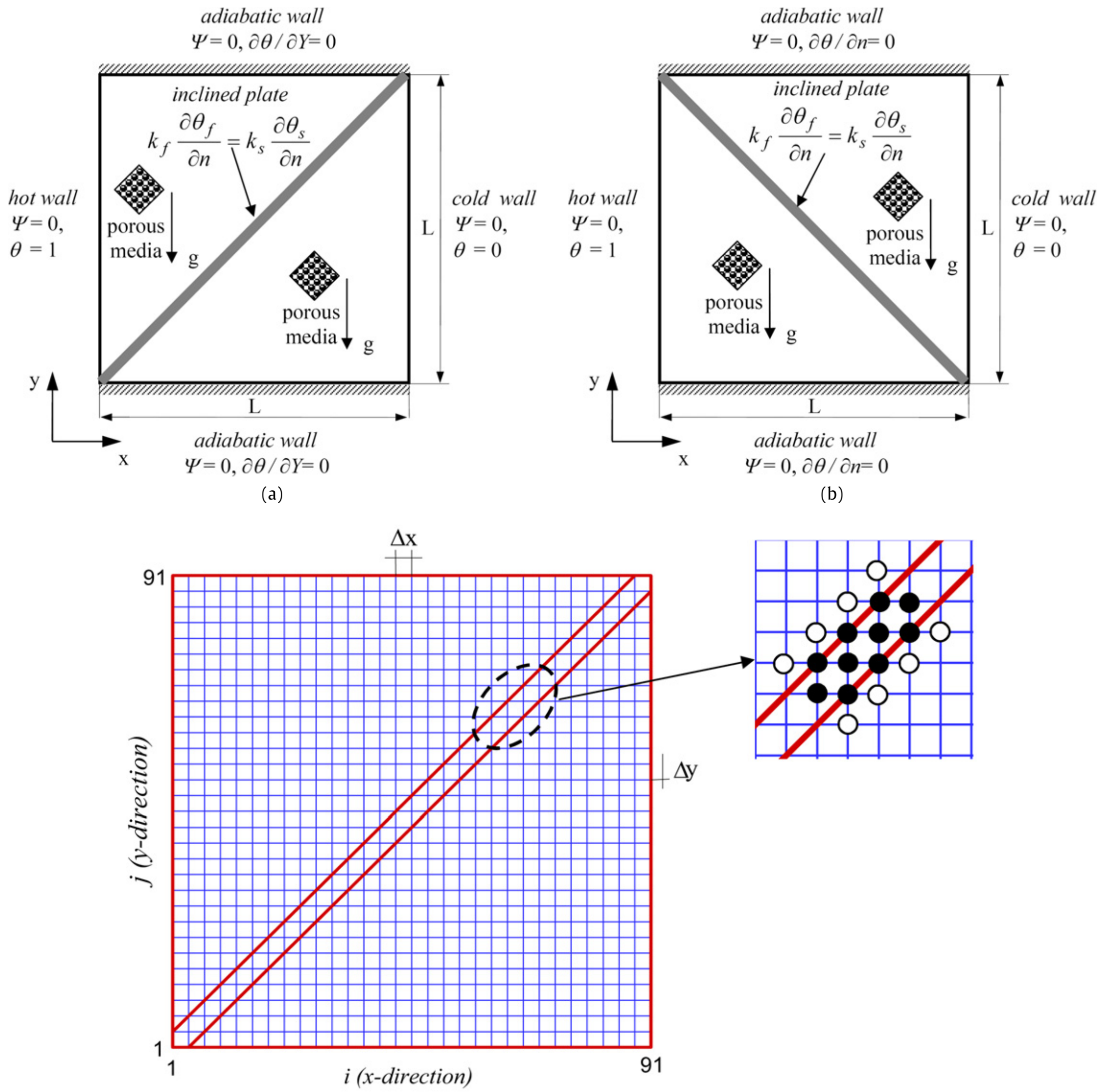

Fig. 1. Physical model: (a) Case I, (b) Case II, (c) finite-difference grids for the cavity.

$$X=\frac{x}{L},\qquad Y=\frac{y}{L},\qquad (U,V)=\frac{(u,v)L}{\alpha_m},\qquad \Psi=\frac{\psi}{\alpha_m}$$
$$\theta_f=\frac{T_f-T_C}{T_H-T_C},\qquad \theta_s=\frac{T_s-T_C}{T_H-T_C} \tag{9}$$

The boundary conditions of Eqs. (6)–(8) are:

for all solid boundaries

$$\Psi=0 \tag{10a}$$

on the left vertical wall (hot), $0\leqslant Y\leqslant 1$

$$\theta_f=\theta_s=1 \tag{10b}$$

on the right vertical wall (cold), $0\leqslant Y\leqslant 1$

$$\theta_f=\theta_s=0 \tag{10c}$$

on the top and bottom walls (adiabatic), $0\leqslant X\leqslant 1$

$$\frac{\partial\theta_f}{\partial Y}=\frac{\partial\theta_s}{\partial Y}=0 \tag{10d}$$

for the interface between the inclined plate and porous media,

$$k_f\frac{\partial\theta_f}{\partial n}=k_s\frac{\partial\theta_s}{\partial n} \tag{10e}$$

where n denotes the normal direction to the inclined plate, k_f is the thermal conductivity of the fluid-saturated porous medium and k_s is the thermal conductivity of the inclined solid plate, respectively. In above boundary condition, the total heat flux q_w is assumed to have the same representation as the case of local thermal equilibrium. In other words, it is assumed that both phases have the same temperature and temperature gradient at the wall as indicated by Alazmi and Vafai [26]. Physical quantities of interest in this problem are the local Nusselt number along the hot wall (Nu_y) and the inclined plate (Nu_ℓ). They are defined as follows

$$Nu_y=\left(-\frac{\partial\theta_f}{\partial X}\right)_{X=0} \tag{11a}$$

$$Nu_\ell=-\frac{\partial\theta_f}{\partial n} \tag{11b}$$

the mean Nusselt number Nu which is given by

$$Nu=\int_0^1 Nu_y\,dy \tag{12}$$

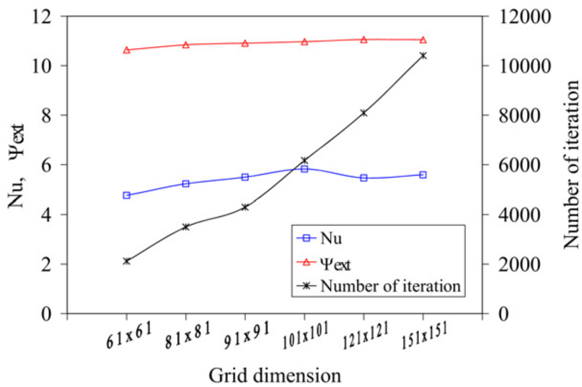

Fig. 2. Grid independency tests.

Table 1
Comparison of the mean Nusselt number for a square porous cavity with results from the literature at $Ra = 1000$.

References	Nu
Bejan [30]	15.800
Cross et al. [31]	13.448
Goyeau et al. [32]	13.470
Manole and Lage [33]	13.637
Baytas and Pop [34]	13.726
Saeid and Pop [35]	14.060
Present result	13.564

3. Method of solution

The numerical method used to solve the system of Eqs. (6)–(7) is the finite-difference method. The solution of linear algebraic equations was performed through the Successive Under Relaxation (SUR) method. Value of 0.1 is taken for under-relaxation parameter for all parameters. The solution domain consists of grid points at which equations are applied. Fig. 2 shows the grid independency result for $k = 1.0$, $Ra = 1000$ and Case I. This figure presents the iteration number, Nusselt number and Ψ_{ext} versus grid dimensions. Care was taken to provide grid independent solutions due to presence of inclined plate. After experimenting with various grid layouts (from 61×61 to 151×151), it was observed that 91×91 is enough for grid independency. Uniform structured mesh was adopted in the current study as given in Fig. 1(c). Beyond this value, the solution needs more iteration. The grid distribution for inclined plate is the most important difficulty for this study. The inclined wall was approximated with staircase-like zigzag lines. As given in Fig. 1(c) that white circles are boundary nodes and they are subject to Dirichlet boundary conditions. Values of internal nodes (black circles) are calculated using boundary values via central difference methods. This technique was used in earlier studies for triangular enclosures by Haese and Teubner [27], and Asan and Namli [28] and for trapezoidal enclosure by Varol et al. [29]. Distance between nodes is shown by ΔX and ΔY in X- and Y-directions, respectively. The iteration process is terminated when the following condition is satisfied:

$$\sum_{i,j}\left|\Phi_{i,j}^{m}-\Phi_{i,j}^{m-1}\right| \Big/ \sum_{i,j}\left|\Phi_{i,j}^{m}\right| \leqslant 10^{-5} \tag{13}$$

where Φ stands for either θ or Ψ, and m denotes the iteration step.

4. Code validation

Due to lack of suitable results in the literature pertaining to the present configuration, the present results have been validated against the existing results for a square cavity filled with a porous medium. The obtained numerical results are compared with those given by different authors in Table 1 (Bejan [30], Gross et al. [31], Goyeau et al. [32], Manole and Lage [33], Baytas and Pop [34], and Saeid and Pop [35]) for a differentially heated square cavity with adiabatic horizontal sides. But different methods were used in literature for same problem. As it can be seen from Table 1, the obtained results show good agreement with the results of the literature. Therefore, it can be concluded that the present numerical method can be used with great confidence to study the problem discussed in this paper.

5. Results and discussion

A numerical study has been performed to investigate the natural convection in diagonally divided square enclosures filled with porous media for different values of the Rayleigh number, thermal conductivity ratio and position of the divided plate inside the cavity.

5.1. Flow field and temperature distributions

Fig. 3 illustrates the streamlines (on the left) and isotherms (on the right) for Case I when $k = 1.0$ at different Rayleigh numbers. Two isosceles triangular enclosures were formed due to presence of the diagonally located plate. At low values of the Rayleigh num-

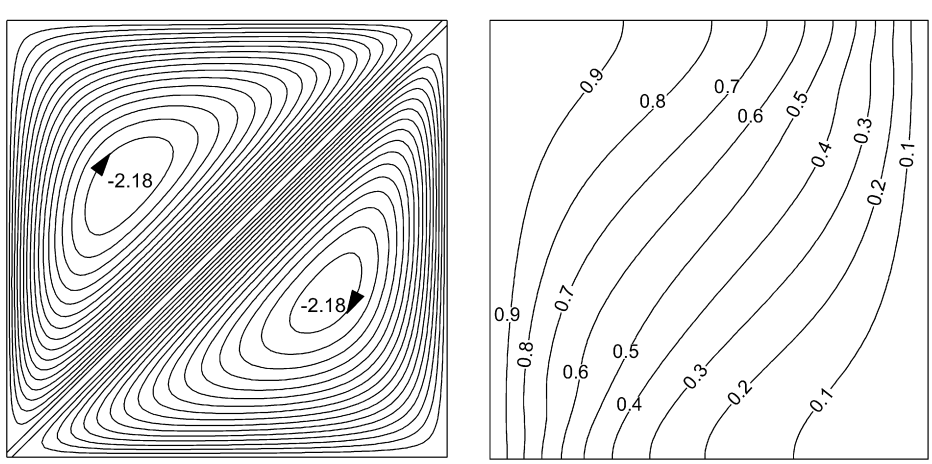

(a)

Fig. 3. Streamlines (left) and isotherms (right) for Case I and $k = 1.0$: (a) $Ra = 100$, (b) $Ra = 250$, (c) $Ra = 500$, (d) $Ra = 1000$.

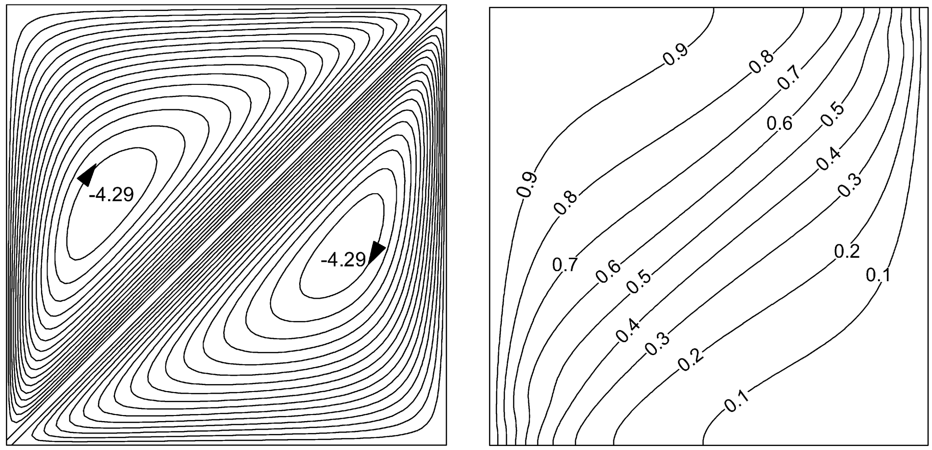

(b)

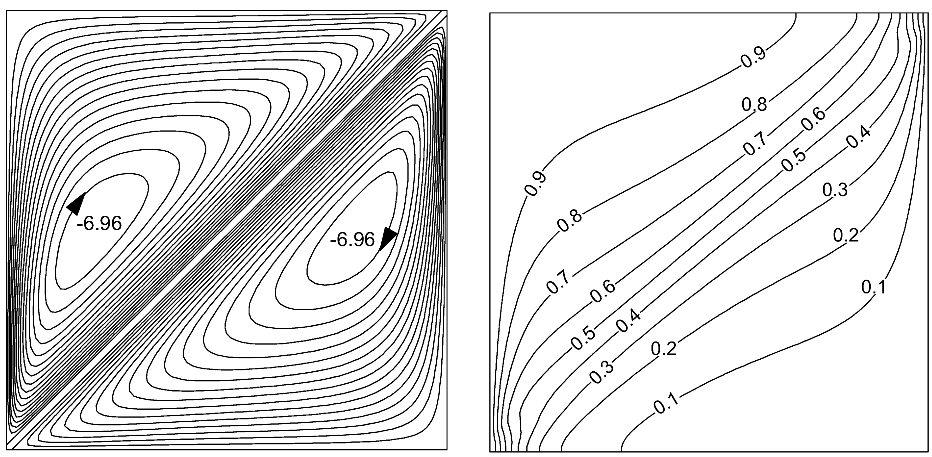

(c)

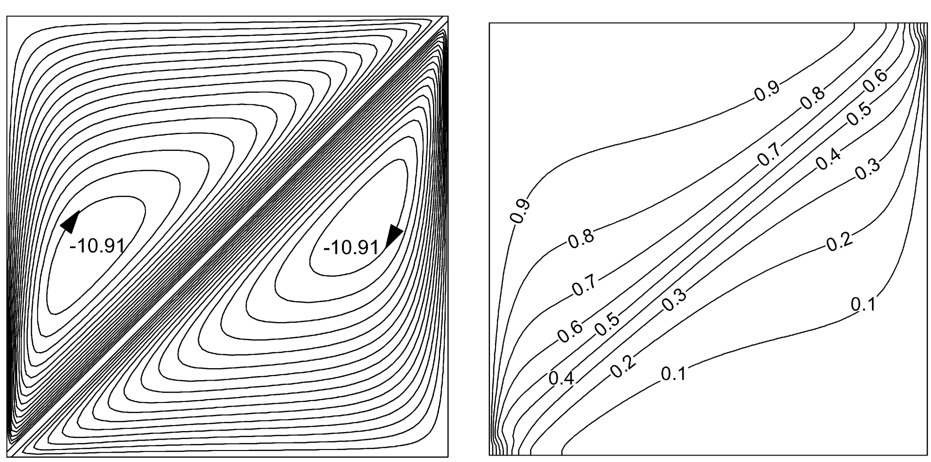

(d)

Fig. 3. (*continued*)

ber, Fig. 3(a), isotherms on the right shows a conduction regime. Flow field is symmetric according to partition and single cell is formed in each of the partitioned enclosures. Both left and right cells rotate in clockwise direction with $\psi_{\min} = -2.18$. In other words, there is a weak clockwise circulation due to domination of conduction. Fig. 3(b) shows that the circulation is more vigorous and center of left and right cells move left bottom and right top corner, respectively. In this case, value of minimum stream function is $\psi_{\min} = -4.29$. It means that when Rayleigh is increased a weak circulation starts, owing to hot vertical wall. The warmer fluid lifted by the gravitational force induced by the horizontal temperature gradient due to the hot wall meets the descending colder fluid layer in the vicinity of the partition. For higher Rayleigh numbers, Figs. 3 (c) and (d), the convection is vigorous with $\psi_{\min} = -6.96$ and $\psi_{\min} = -10.91$, respectively. Increasing of Rayleigh numbers also increase the interaction between hot and cold walls and cell moves toward the corners in both region of the partition. Isotherms become steeper with increasing of Rayleigh number at isotherm walls. They are more clustered around the partition for higher Rayleigh numbers.

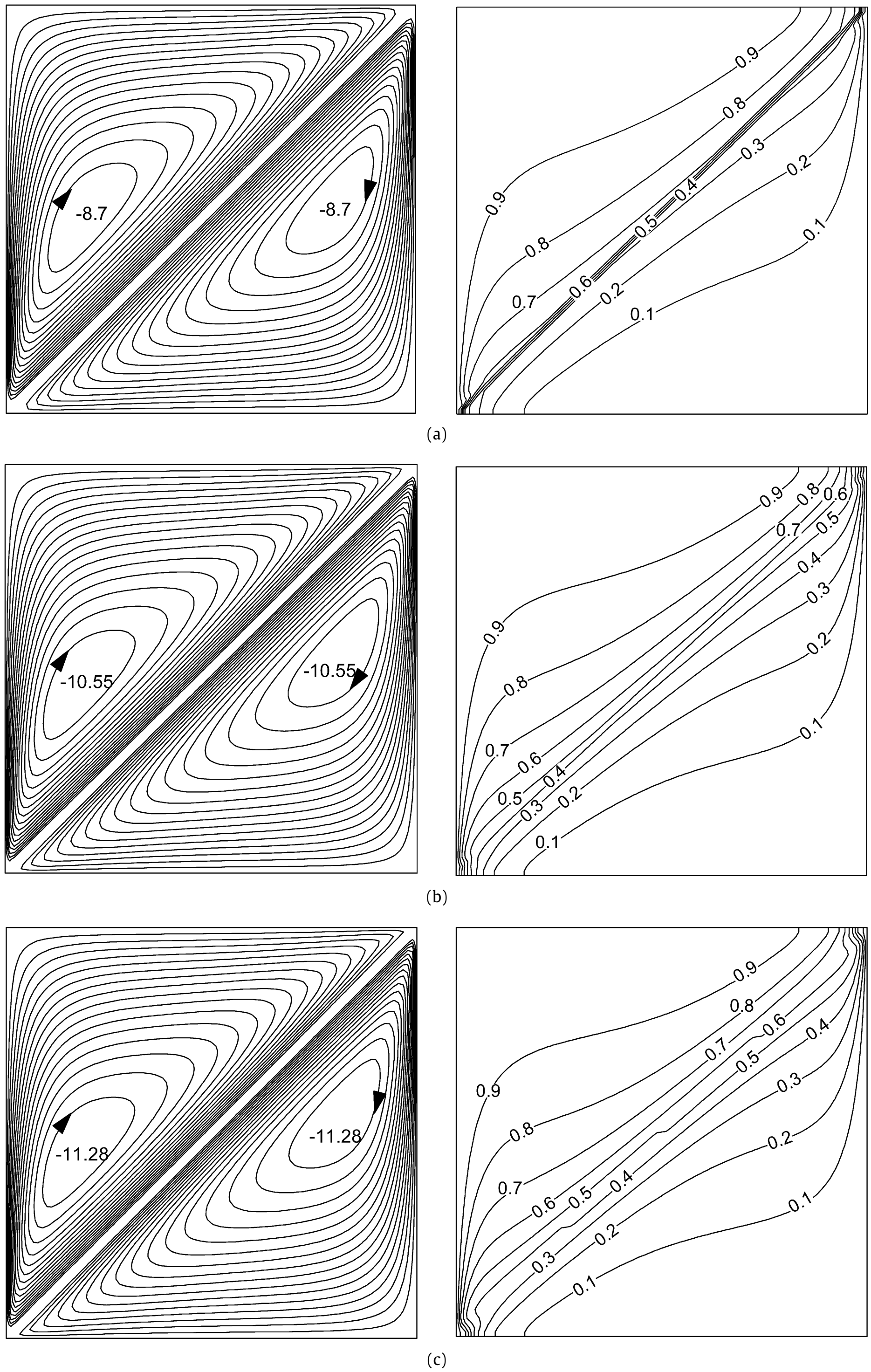

Fig. 4. Streamlines (left) and isotherms (right) for Case I and $Ra = 1000$: (a) $k = 0.1$, (b) $k = 0.5$, (c) $k = 10$.

Figs. 4 and 3(d) show the streamlines and isotherms to show the effects of thermal conductivity ratio on flow fields and temperature distribution for Case I and $Ra = 1000$. Flow strength increases with increasing of thermal conductivity ratio due to increasing of heat transfer from hot wall to cold. $|\psi_{\min}|$ values are changed as 8.7, 10.55 and 11.28 for $k = 0.1, 0.5$ and 10, respectively. The center of cells moves toward the corners depends on thermal conductivity. Isotherms are clustered around the inclined partition due to higher thermal conductivity of the partition. Thus, the medium at left top and right bottom corner becomes uniform. Thermal effectiveness of the plate decreases with the increasing of thermal conductivity and temperature gradient becomes smaller with increasing of thermal conductivity ratio. Finally, convection mode of heat transfer increases with increasing of thermal conductivity.

Results of streamlines (left) and isotherms (right) are presented in Fig. 5 for Case II and $k = 1.0$. The figure can be compared with Fig. 3 to show the effects of position of inclined partition on thermal and flow field. In this case, inclination angle for inclined plate changes and again, two triangular enclosures were formed. But shape of cells is affected from the changing of inclination angle of

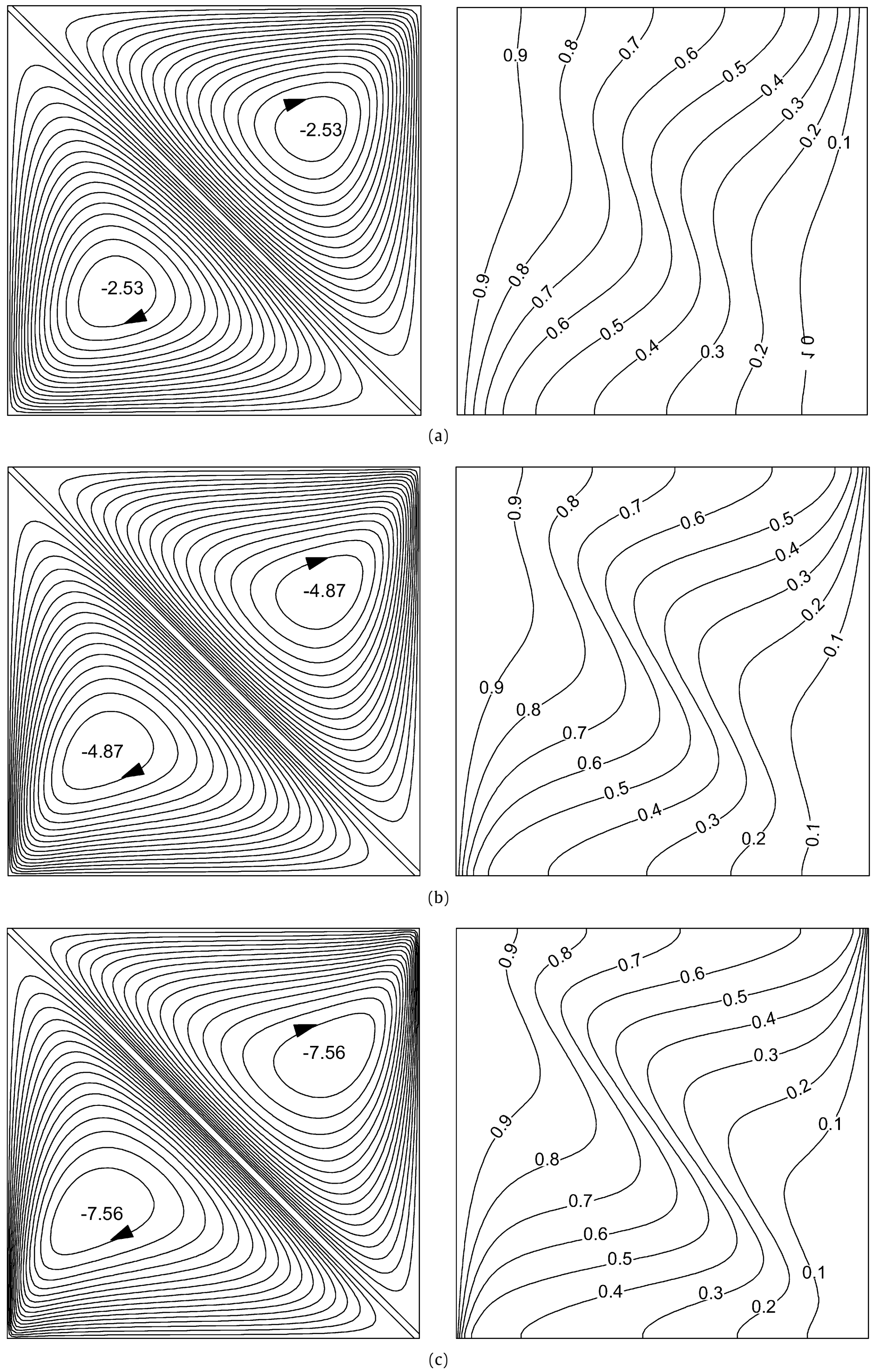

Fig. 5. Streamlines (left) and isotherms (right) for Case II and $k = 1.0$: (a) $Ra = 100$, (b) $Ra = 250$, (c) $Ra = 500$, (d) $Ra = 1000$.

the partition. From the physical aspect, the distance for heat transfer becomes shorter from heated wall to partition. Length and flow strength of main cell increases with increasing of Rayleigh number. The left one is heated from left vertical wall and heat is transferred from inclined wall. The upper one is heated from inclined wall and cooled from vertical wall. The cells rotate in clockwise direction in both enclosures. Isotherms show wavy distribution for all cases. But amplitude of each isotherm changes with Rayleigh numbers.

Fig. 6 shows the effects of thermal conductivity on natural convection for Case II and $Ra = 1000$. Even though there is discernible difference in streamlines for different values of thermal conductivity ratio, absolute value of minimum stream function value show that the convection has increased with increasing k. As shown from the figure that values of $\psi_{\min}$ are -8.98, -10.88 and -11.7 for $k = 0.1, 0.5$ and 10, respectively. In this problem the parameter of k is chosen as thermal conductivity ratio of fluid to thermal conductivity of inclined plate. When figure compares with Fig. 4, Case I, the distribution of isotherms are completely different. The reason is: The way of heat transfer becomes different due to location direction of the partition.

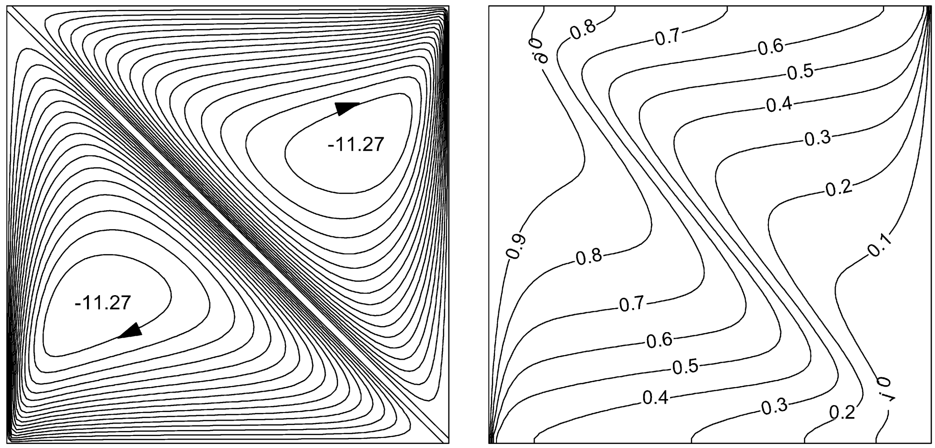

(d)

Fig. 5. (*continued*)

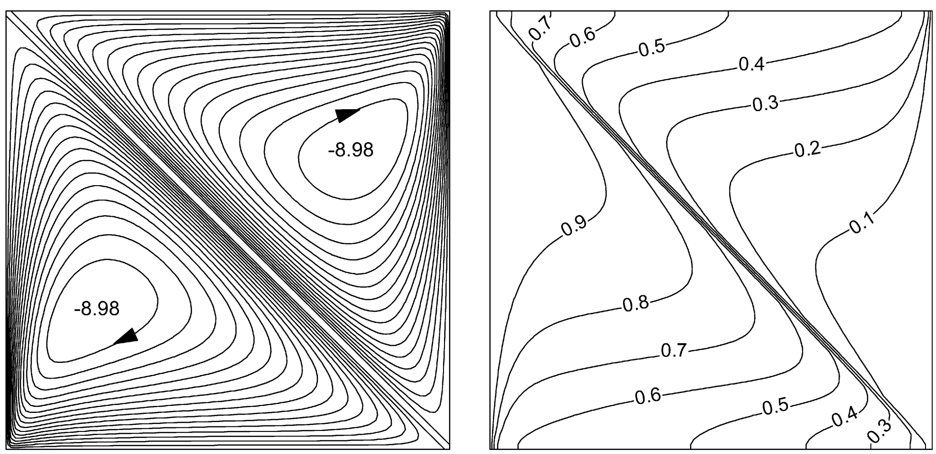

(a)

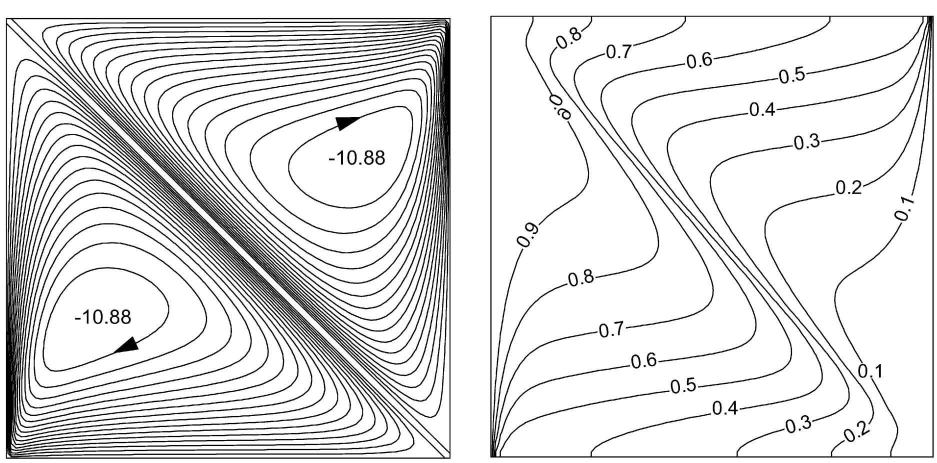

(b)

Fig. 6. Streamlines (left) and isotherms (right) for Case II and $Ra = 1000$: (a) $k = 0.1$, (b) $k = 0.5$, (c) $k = 10$.

5.2. Heat transfer

Heat transfer as a function of various parameters is evaluated and presented as the local and mean Nusselt numbers. Calculation of local Nusselt numbers for hot wall and inclined plate is given by Eqs. (11a) and (11b), respectively. And mean Nusselt number is calculated using Eq. (12).

Variation of local Nusselt number is shown in Figs. 7 (a) and (b) at $k = 1.0$ for different Rayleigh numbers along the hot and cold walls, respectively. Heat transfer increases with increasing of Rayleigh number for both Cases I and II. But lower Nusselt number is formed in Case I due to increasing of volume of the fluid between hot wall and partition. Thus, the distance between them is increased and heat transfer decreases. For Case I, heat transfer increases at the lower end of the partition up to $Y \approx 0.1$ then it decreases. At this part of the partition, there is a strong heat transfer between vertical wall and partition due to short distance. On

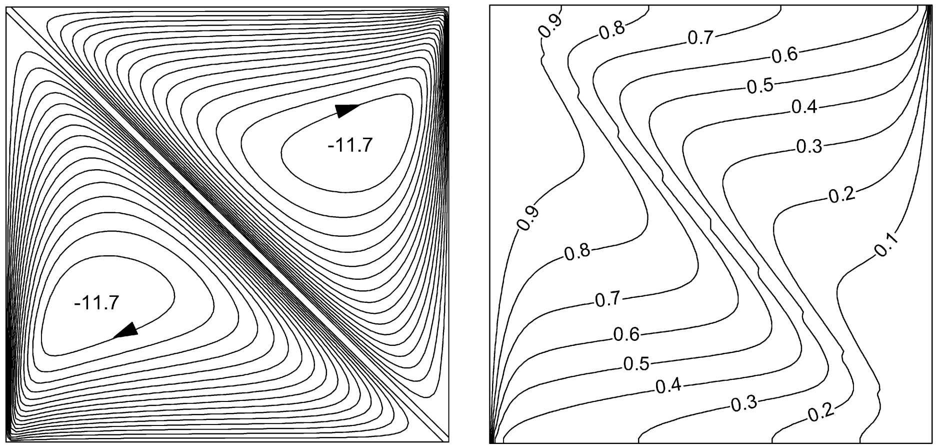

(c)

Fig. 6. (*continued*)

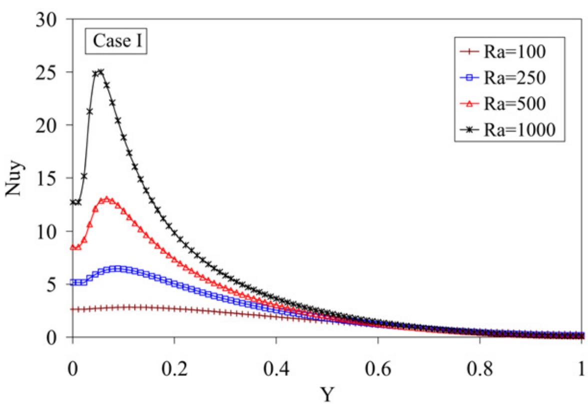

(a)

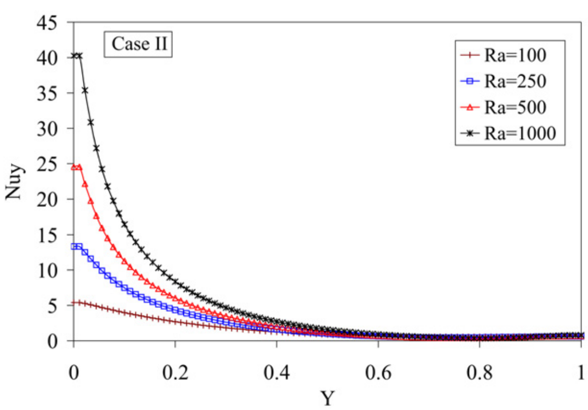

(b)

Fig. 7. Variation of local Nusselt number along the hot wall at $k = 1.0$ for different Rayleigh numbers: (a) Case I, (b) Case II.

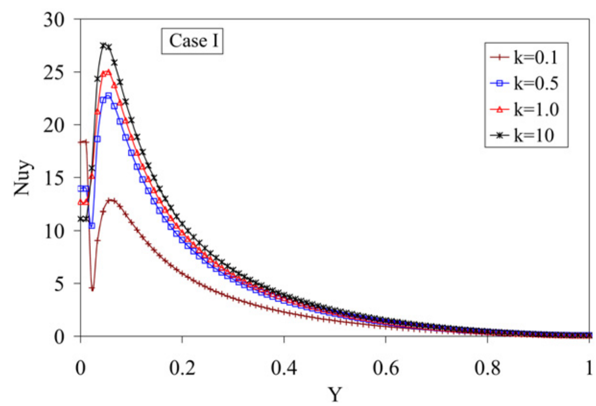

(a)

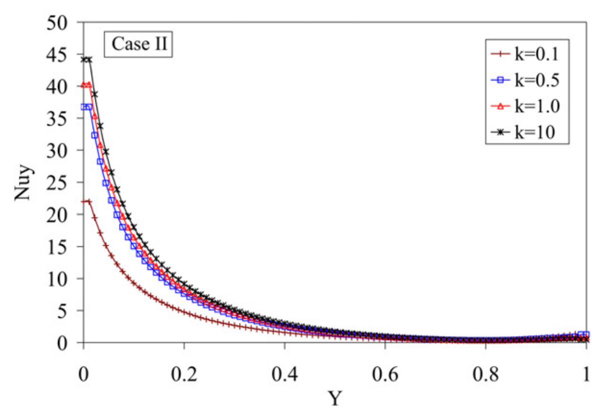

(b)

Fig. 8. Variation of local Nusselt number along the hot wall at $Ra = 1000$ for different thermal conductivity ratios: (a) Case I, (b) Case II.

the contrary, the local Nusselt number has a maximum value and decreases along the wall. It means that the fluid becomes motionless and conduction mode of heat transfer increases. The value of Nusselt number equals almost 1 at this part of the wall.

Effects of thermal conductivity ratio on variation of local Nusselt numbers are given in Figs. 8 (a) and (b) for Cases I and II, respectively. It is seen that Nusselt number is an increasing function of thermal conductivity ratio for both cases. However, trend is different. However, trend is different. In Case I, local Nusselt number is very low at the left corner due to presence of inclined plate. It increases suddenly above the plate and it decreases. Due to motionless fluid at the top of the enclosure heat transfer becomes extremely weak. It should be noted that the partition contacts the vertical surfaces at small segment. At those two segments the porous medium is not adjacent to the surface, hence, Eq. (11a) cannot be used there unless $k = 1.0$. By noting Eq. (10e), the general form for Nu_y is $Nu_y = (-\frac{k_i}{k_f}\frac{\partial \theta_i}{\partial n})_{n=+}$, where "$i$" is the index for medium adjacent to the surface (or plate) and can be "f" or "s".

Figs. 9 and 10 illustrate the variation of local Nusselt number along the inclined plate for different Rayleigh numbers at Cases I and II, respectively. Values are obtained from the heated region of the plate. In this context, Fig. 9(a) shows the results for different

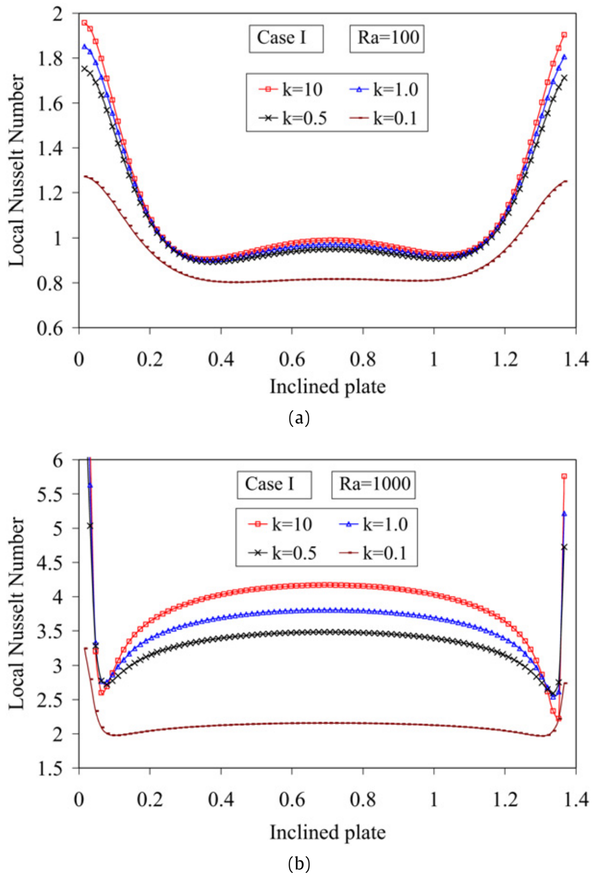

Fig. 9. Variation of local Nusselt number along the inclined plate for Case I, (a) $Ra = 100$, (b) $Ra = 1000$.

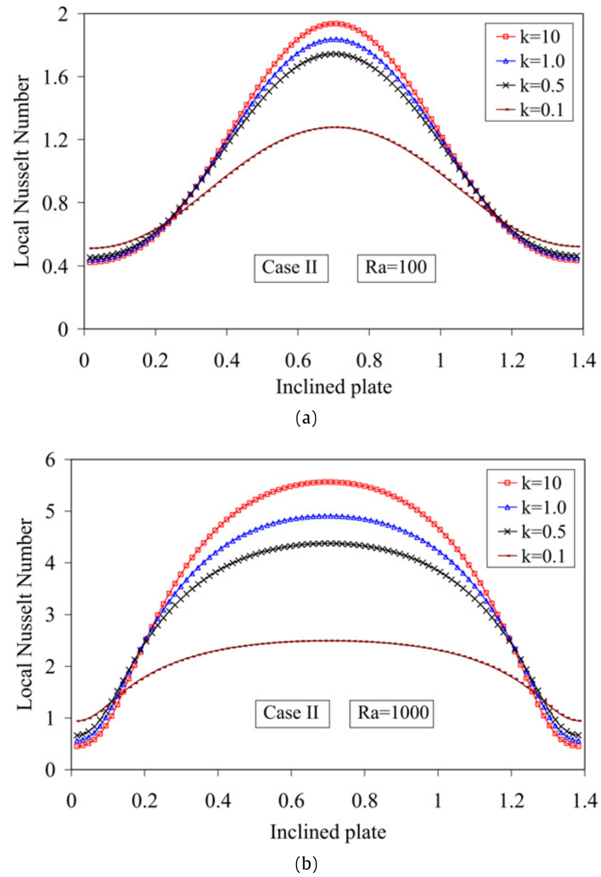

Fig. 10. Variation of local Nusselt number along the inclined plate for Case II, (a) $Ra = 100$, (b) $Ra = 1000$.

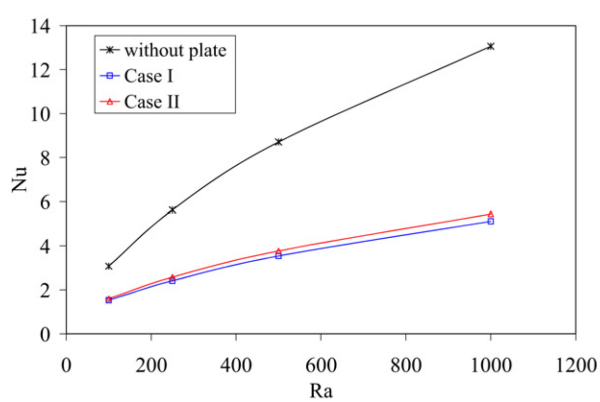

Fig. 11. Variation of the mean Nusselt number with Rayleigh number for different cases.

thermal conductivity values at $Ra = 100$ and Case I. As seen from the figure that values are very close to each other for $k \geqslant 1$. In this case, the partition is more conductive and higher heat transfer is former. At the lower and upper part of the partition, higher heat transfer is observed due to increasing of thermal conductivity of the plate. At this region, the distance between hot wall and partition is very close to each other. Local Nusselt number becomes constant along the inclined plate for $k < 1$. It means that the partition behaves a curtain for heat transport. Comparison of Figs. 9 (a) and (b) gives that values of local Nusselt number increases with increasing of Rayleigh number, as expected. With the increase of Rayleigh number, more energy inputs into the system. Thermal conductivity value becomes more effective for higher Rayleigh numbers and its value increases with increasing of thermal conductivity. As indicated above that the local Nusselt number is calculated from the heated side of the inclined plate using Eq. (11b). Results for cold side of the partition are not shown here but it is obtained same value due to small thickness of the partition. The heat transfer becomes maximum near the middle part of the inclined plate. It is due to the fact that heat transport way becomes normal to the partition at the point. Heat transfer becomes maximum near the attachment point of the partition due to higher heat transfer between hot wall and inclined plate. Figs. 10 (a) and (b) is given to make comparison of variation of local Nusselt number for both cases. The figure shows that trend of local Nusselt number is completely different between two cases especially at attachment points. A bell-shaped trend is formed for local Nusselt numbers along the inclined plate. Values are decreased with decreasing of thermal conductivity values for both $Ra = 100$ and 1000. The bell-shape becomes wider for higher Rayleigh numbers. It means that lower and upper effects of the partition are reduced. Overall comparison of Figs. 9 and 10 indicate that higher local Nusselt number values are formed at the middle point of the partition for Case II.

Both Fig. 11 and Table 2 summarize the effect of insertion of inclined partition on heat transfer inside the enclosure. Thus, Fig. 11 shows the variation of mean Nusselt number with Rayleigh number for both cases and the enclosure without partition. Mean Nusselt number increases almost linearly with increasing of Rayleigh number for all situations. Higher heat transfer was formed in Case II than that of Case I. But in both cases, inclined plate reduces the heat transfer. Table 2 presents the Percent Reduction (PR) which is defined by Eq. (14) for both bisected enclosure and non-partitioned enclosures (Tong and Gerner [7]). In this equation, *Nu* depicts the Nusselt number for the actual case being examined

Table 2
Comparisons of percent reduction (PR) of heat transfer.

Ra	Mean Nusselt number (Nu)			Percent reduction in heat transfer (%) $\mathrm{PR} = [\frac{Nu_0 - Nu}{Nu_0}] \times 100$	
	Without plate	Case I	Case II	Case I	Case II
100	3.081	1.530	1.601	50.32	48.02
250	5.630	2.417	2.581	57.07	54.16
500	8.712	3.548	3.771	59.27	56.71
1000	13.564	5.122	5.449	60.79	58.29

(with partition), and Nu_0, Nusselt number for a non-partitioned enclosure having the same dimensions and governing parameters. As seen from the figure that heat transfer decreases with the presence of orthogonally located plate for both cases. The table also shows that Nusselt number is a strong function of position of the plate. More reducing on heat transfer is formed by Case I

$$\mathrm{PR} = \left[\frac{Nu_0 - Nu}{Nu_0}\right] \times 100 \tag{14}$$

6. Conclusion

Laminar natural convection in divided square enclosures filled with fluid-saturated porous media divided by an diagonally located thin plate has been studied numerically. Finite difference method was used to solve governing equations. Results were obtained for two different cases based on inclination angle of plate as 45°, Case I and 135°, Case II. The Rayleigh number changes in the range of $100 \leqslant Ra \leqslant 1000$. The obtained results showed that:

(a) Heat transfer reduces with insertion of the inclined plate irregardless of the position and Rayleigh number.
(b) Heat transfer and flow field are strongly depended on position of the plate. Higher heat transfer was formed at Case II than that of Case I.
(c) Higher heat transfer is formed at the middle of the inclined plate for both cases.
(d) Symmetric flow field was observed for all parameters at the both chest inside the enclosure in both cases. For all cases, flow rotates in clockwise circulation direction.

References

[1] D.A. Nield, A. Bejan, Convection in Porous Media, 3rd ed., Springer, New York, 2006.
[2] D.B. Ingham, I. Pop (Eds.), Transport Phenomena in Porous Media III, Elsevier, Oxford, 2005.
[3] K. Vafai (Ed.), Handbook of Porous Media, 2nd ed., Taylor & Francis, New York, 2005.
[4] I. Pop, D.B. Ingham, Convective Heat Transfer: Mathematical and Computational Modeling of Viscous Fluids and Porous Media, Pergamon, Oxford, 2001.
[5] A. Bejan, I. Dincer, S. Lorente, A.F. Miguel, A.H. Reis, Porous and Complex Flow Structures in Modern Technologies, Springer, New York, 2004.
[6] P. Vadasz (Ed.), Emerging Topics in Heat and Mass Transfer in Porous Media, Springer, New York, 2008.
[7] T.W. Tong, F.M. Gerner, Natural convection in partitioned air-filled rectangular enclosures, Int. Comm. Heat Mass Transfer 13 (1986) 99–108.
[8] C.J. Ho, Y.L. Yih, Conjugate natural convection heat transfer in an air-filled rectangular cavity, Int. Comm. Heat Mass Transfer 14 (1987) 91–100.
[9] T. Nishimura, M. Shiraishi, Y. Kawamura, Natural convection heat transfer in enclosures with an off-center partition, Int. J. Heat Mass Transfer 30 (1987) 1756–1758.
[10] H. Turkoglu, N. Yucel, Natural convection heat transfer in enclosures with conducting multiple partitions and side walls, Heat and Mass Transfer 32 (1996) 1–8.
[11] K.S. Chen, A.C. Ku, C.H. Chou, Investigation of natural convection in partially divided rectangular enclosures both with and without an opening in the partition plate: Measurement results, J. Heat Transfer 112 (1990) 648–652.
[12] E. Bilgen, Natural convection in enclosures with partial partitions, Ren. En. 26 (2002) 257–270.
[13] H.F. Oztop, I. Dagtekin, Natural convection heat transfer by heated partitions within enclosures, Int. Comm. Heat Mass Transfer 28 (2001) 823–834.
[14] M.W. Nanstell, R. Greif, Natural convection in undivided and partially divided rectangular enclosures, J. Heat Transfer 103 (1981) 623–629.
[15] M.W. Nanstell, R. Greif, An investigation of natural convection in enclosures with two and three dimensional partitions, Int. J. Heat Mass Transfer 27 (1984) 561–571.
[16] Y. Varol, H.F. Oztop, A. Varol, Effects of thin fin on natural convection in porous triangular enclosures, Int. J. Therm. Sci. 46 (2007) 1033–1045.
[17] Y. Varol, H.F. Oztop, Control of buoyancy-induced temperature and flow fields with an embedded adiabatic thin plate in porous triangular cavities, Appl. Therm. Sci. 29 (2009) 358–366.
[18] N.H. Saeid, Conjugate natural convection in a porous enclosure: effect of conduction in one of the vertical walls, Int. J. Thermal Sci. 46 (2007) 531–539.
[19] N.H. Saeid, Conjugate natural convection in a vertical porous layer sandwiched by finite thickness walls, Int. Comm. Heat Mass Transfer 34 (2007) 210–216.
[20] D.A. Nield, A.V. Kuznetsov, Local thermal nonequilibrium effects in forced convection in a porous medium channel: a conjugate problem, Int. J. Heat Mass Transfer 42 (1999) 3245–3252.
[21] A. Ben-Nakhi, A.J. Chamkha, Conjugate natural convection in a square enclosure with inclined thin fin of arbitrary length, Int. J. Therm. Sci. 46 (2007) 467–478.
[22] A. Ben-Nakhi, A. Chamkha, Effect of length and inclination of a thin fin on natural convection in a square enclosure, Numer. Heat Transfer Part A 50 (2006) 389–407.
[23] A. Mezrhab, M. Jami, C. Abid, M. Bouzidi, P. Lallemand, Lattice-Boltzmann modelling of natural convection in an inclined square enclosure with partitions attached to its cold wall, Int. J. Heat Fluid Flow 27 (2006) 456–465.
[24] M. Jami, A. Mezrhab, M. Bouzidi, P. Lallemand, Lattice-Boltzmann computation of natural convection in a partitioned enclosure with inclined partitions attached to its hot wall, Physica A 368 (2006) 481–494.
[25] B. Sahin, M.E. Arici, Kapalı kare ortamlarda yatay, düşey ve eğik iç bölmelerin doğal taşınımla ısı transferine etkisinin sayısal incelenmesi, in: Proceedings of ULIBTK'05, Heat Science Congress 2 (2005) 789–794 (in Turkish).
[26] B. Alazmi, K. Vafai, Analysis of fluid flow and heat transfer interfacial conditions between a porous medium and a fluid layer, Int. J. Heat Mass Transfer 44 (2001) 1735–1749.
[27] P.M. Haese, M.D. Teubner, Heat exchange in an attic space, Int. J. Heat Mass Transfer 45 (2002) 4925–4936.
[28] H. Asan, L. Namli, Numerical simulation of buoyant flow in a roof of triangular cross-section under winter day boundary conditions, Energy & Buildings 33 (2001) 753–757.
[29] Y. Varol, H.F. Oztop, I. Pop, Numerical analysis of natural convection in an inclined trapezoidal enclosure filled with a porous medium, Int. J. Therm. Sci. 47 (2008) 1316–1331.
[30] A. Bejan, On the boundary layer regime in a vertical enclosure filled with a porous medium, Lett. Heat Mass Transfer 6 (1979) 93–102.
[31] R.J. Gross, M.R. Bear, C.E. Hickox, The application of flux-corrected transport (FCT) to high Rayleigh number natural convection in a porous medium, in: Proc. 8th Int. Heat Transfer Conf., San Francisco, CA, 1986.
[32] B. Goyeau, J.P. Songbe, D. Gobin, Numerical study of double-diffusive natural convection in a porous cavity using the Darcy–Brinkman formulation, Int. J. Heat Mass Transfer 39 (1996) 1363–1378.
[33] D.M. Manole, J.L. Lage, Numerical benchmark results for natural convection in a porous medium cavity, in: Heat and Mass Transfer in Porous Media, ASME Conference, HTD, vol. 216, 1992, pp. 55–60.
[34] A.C. Baytas, I. Pop, Free convection in oblique enclosures filled with a porous medium, Int. J. Heat Mass Transfer 42 (1999) 1047–1057.
[35] N.H. Saeid, I. Pop, Natural convection from a discrete heater in a square cavity filled with a porous medium, J. Porous Media 8 (2005) 55–63.